

## Application of terahertz technology in nondestructive testing of ceramic matrix composite defects

Zhou Xiaodan, Li Lijuan, Zhao Duo, Ren Jiaojiao

(School of Opto-electronic Engineering, Changchun University of Science and Technology, Changchun 130022, China)

**Abstract:** Ceramic Matrix Composite (CMC) has been widely applied for its excellent protection performance. It was hard for traditional testing means as ultrasonic to complete internal inspection due to the porous structure of CMC. Terahertz Time-Domain Spectroscopy (THz-TDS) was applied to establish the THz Nondestructive Testing (NDT) model of thickness at single point and to extract optical parameters of material samples. In further verifying experiments, exploratory detection and evaluation were developed on porosity distribution and defect sizes. Scanning imaging performance and conclusion of time-frequency spectrum analysis are relatively plausible on CMC internal testing through the experiments. The study in this paper proves the revealing ability of THz-TDS on quantitative NDT and properties exploring of specific materials.

**Key words:** terahertz time-domain spectroscopy; ceramic matrix composite; nondestructive testing; quantitative detection

**CLC number:** O433.4    **Document code:** A    **DOI:** 10.3788/IRLA201645.0825001

## 太赫兹技术在陶瓷基复合材料缺陷无损检测中的应用

周小丹, 李丽娟, 赵 铎, 任姣姣

(长春理工大学 光电工程学院, 吉林 长春 130022)

**摘 要:** 太赫兹时域光谱技术(THz-TDS)是一种通过宽频带太赫兹脉冲携带介质信息,从而完成对样品内部信息提取的无损检测技术。目前,这种技术大多应用于安全监测,外形成像等定性分析领域。将该应用广泛的陶瓷基复合材料做为检测样品,通过建立单点厚度检测模型和光学参数的提取,将该技术用于密度分布检测和孔洞缺陷尺寸检测,进行定量测量。设计并进行了验证实验,对标准材料及缺陷进行了探索性的测量及评价。实验获取了较为理想的时频光谱分析结果及成像结果,显示出了 THz-TDS 在材料的定量无损检测和探究材料特征方面具有揭示作用。

**关键词:** THz-TDS; 陶瓷基复合材料; 无损检测; 缺陷定量分析

收稿日期:2015-12-05; 修订日期:2016-01-03

作者简介:周小丹(1990-),女,硕士生,主要从事太赫兹无损检测方面的研究。Email:15043055626@163.com

导师简介:李丽娟(1972-),女,教授,博士生导师,博士,主要从事仪器科学与技术方面的研究。Email:custjuan@126.com

## 0 Introduction

Ceramic Matrix Composite (CMC) has been widely applied in aerospace field for its excellent protection performance. Internal defects may exist due to the cumbersome manufacturing process; as the brittleness of the material, which could easily cause a trauma or even a fracture leading to the final material invalidation when loaded in different directions<sup>[1-2]</sup>. Current research shows that the terahertz wave has a good permeability for CMC. The absorption is rather obvious between the frequencies of 0.1-3THz. According to the research of NASA's Marshall Space Flight Center, plausible results have been achieved in CMC Nondestructive Testing (NDT) with Terahertz Time-Domain Spectroscopy (THz-TDS)<sup>[3-5]</sup>.

Terahertz technology concludes THz-TDS and Terahertz imaging technology ect. THz imaging technology<sup>[6]</sup> uses T-Ray radiate the tested object, obtains the information of the object by means of transmission or reflection, and then imaging. THz-TDS is a fire-new spectral technique based on broadband femtosecond laser pulse<sup>[7]</sup>. It is currently applied to qualitative analysis as a means of security detection and material identification. This technology is able to carry medium information of flight path by amplitude variation and time delay of THz pulse during the transmission and reception, so that the internal defect detection of the samples could be both qualitative and quantitative. Different from traditional testing methods, THz-TDS needs to obtain the absorption peak of the material on the frequency band. Then the model of thickness to extract required and optical parameters can be established, after that solutions can be designed for various types of detection, establishing a rational evaluation system. Afterwards, the appropriate computing approach could be selected to form an image of intensity distribution by scanning according to the test results. Finally, accurate and reliable results would be given based on the spectral analysis of time

domain and frequency domain on the characteristic location.

## 1 Detecting model of single point & absorption spectra

### 1.1 Establishing detecting model at single point

THz wave acts basically the same as electromagnetic wave when spreading through materials. A sample to be detected will bring the THz wave passing through a certain amount of time delay compared with an air layer which is the same in thickness because of their different refractive indexes. Also, there is obvious absorption when THz pulse spreads through a CMC sample. The absorption changes linearly with geometric thickness of the detecting point on the sample. So, both the time delay and the amplitude absorption can be taken as an important basis for the quantitative detection.

In the progress of THz NDT, In-homogeneous surface roughness distribution of the material could cause scattering which imports error. Thus both the time delay and the amplitude absorption should be considered when establishing the detection model in experiment.

Shown in Fig.1, the terahertz pulse received after spread through air is represented by  $E_{ref}$ , the pulse received when a sample is placed between the transmitter and the receiver is represented by  $E_{sam}$ .

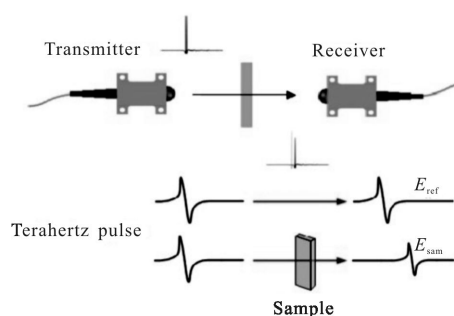


Fig.1 Transmission sketch of terahertz

With the assumption that the sample being tested is a homogeneous unadulterated block with two flat and parallel sides. Our transmitting detect model at

single point could be established as the equation below according to the basic law of geometrical optics.

$$d = \frac{c}{n - n_0} (T_{\text{sam}} - T_{\text{ref}}) = \frac{c}{n - n_0} \Delta T \quad (1)$$

Where  $n_0$  is the refractive index of air and  $n$  is the refractive index of the sample,  $d$  is the thickness of sample,  $T_{\text{sam}}$  is the flight time of sample,  $T_{\text{ref}}$  is the flight time of reference.

Similarly, another equation could be established including a parameter of absorption coefficient as following.

$$E_{\text{sam}} = E_{\text{air}} (1 - e^{-j(\alpha - \alpha_0)d}) \quad (2)$$

Where  $E_{\text{sam}}$  and  $E_{\text{air}}$  refer to the amplitude of the received Terahertz pulses with a sample and just air between the transmitter and the receiver, respectively.  $\alpha_0$  is the absorption coefficient of air, while  $\alpha$  is the absorption coefficient of the sample.

### 1.2 Acquisition of the absorption spectra

Frequency distribution of the detect pulse could be obtained by Fourier transform of terahertz time-domain spectrum<sup>[9]</sup>. The purpose of the Fourier transform is to find out the main frequency of vibration from chaotic signals.

The application of continuous Fourier transform is limited because most of signals to be process in practice are discrete in time sequence. Therefore, using discrete Fourier transform to analysis the frequency response of discrete time sequence signals should be valued.

Fourier transform is done to the received pulse spread through the sample. Compared with the reference pulse which spreads though air, the area of frequency where the absorption taken place could be found.

In Fig.2, the absorption is most obvious in the area between 0.2–1.7 THz<sup>[9]</sup>. This region could be chosen as the interest region in imaging. Extracting the fingerprint spectrum of particular material is significant in improving accuracy of detection and distinguishing inclusions.

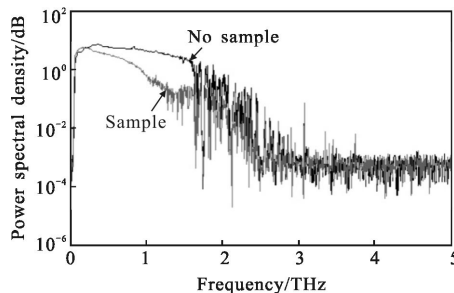


Fig.2 Absorption of the sample in frequency

## 2 Verification experiments

### 2.1 Experimental device

Our THz-TDS device consists of T-GAUGE which is product by Pico Metrix, Transmitter and Receiver. Schematic diagram is shown in Fig.3.

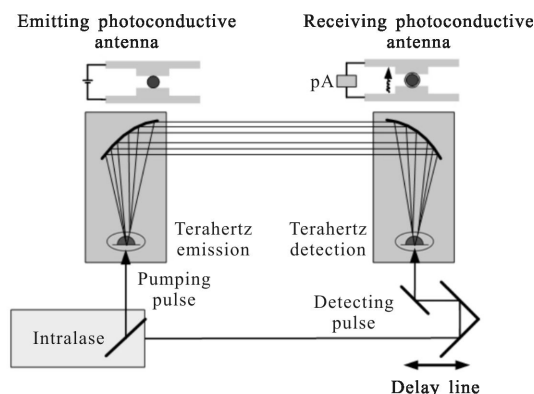


Fig.3 Schematic diagram of the device

Making the motion controlling module and the sampling module corresponding in coordinate by using an X-Y Gantry, as shown in Fig.4, 2D image of intensity distribution could be acquired through detecting information extraction point by point with the data processing module. With the image, the defect could be located efficiently and intuitively.

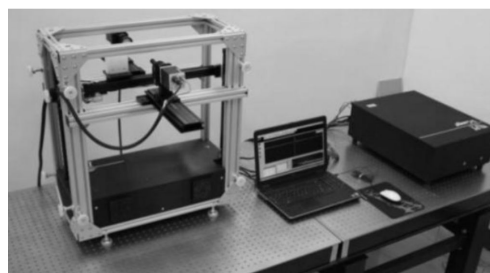


Fig.4 Experimental device

In reflection experiment, a collinear adapter can match up the transmitter and the receiver together and then fit the gantry to reduce the random error.

All experiments in this study are under the conditions of temperature at 26 °C, relative humidity at about 35% to eliminate unnecessary interference.

### 2.2 Evaluation and analysis method of hole-type defects

In quantitative validation experiments, two groups of defects are prefabricated on a piece of CMC sample (85 mm×72 mm×30 mm) shown in Fig.5. The bottoms of the defects are machined quiet roughly, because a smooth plane would supply us with an echo which equals the defect detection to meaningless repeating thickness measurement.

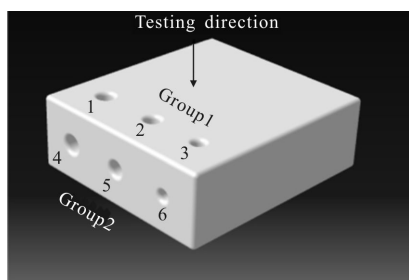


Fig.5 Prefabricated defects sample

The first group is lateral cylindrical hole-type defect:

Defect 1:  $\phi_1=5.5$  nm,  $depth_1=1.5$  nm;

Defect 2:  $\phi_2=5.0$  nm,  $depth_2=2.0$  nm;

Defect 3:  $\phi_3=4.0$  nm,  $depth_3=7.0$  nm;

The second group is transverse cylindrical hole-type defect:

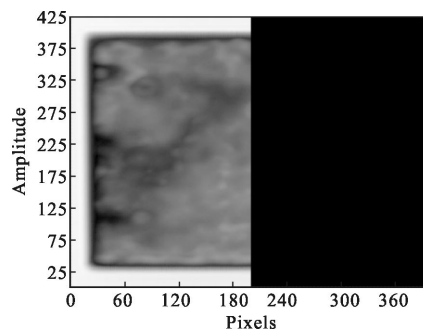
Defect 4:  $\phi_4=6.5$  nm,  $depth_4=7.0$  nm;

Defect 5:  $\phi_5=6.0$  nm,  $depth_5=5.5$  nm;

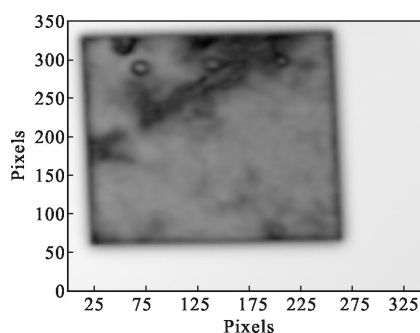
Defect 6:  $\phi_6=4.0$  nm,  $depth_6=4.5$  nm;

Using the two-dimension imaging system to scan the CMC sample under test, we can get point cloud data that carried sample information, then the data is analyzed to obtain THz NDT diagram of the CMC sample. Using X-Y Gantry for scanning, transmission and reflection tests are carried out, and the images are obtained as shown in Fig.6(a) and (b). We can clearly

distinguish the two groups defects of the tested CMC sample from Fig.6.



(a) Transmission image(calculated with time delay)



(b) Reflection image(calculated with power integration in frequency)

Fig.6 THz-TDs imaging

Calculating the time delay and amplitude loss between the waveforms respectively, we can get the depth of defects according to the parameters-extracted and detection model established in the paper above mentioned. We calculate the defects size of the two groups which are based on the reflection of THz – TDS, and take THz-TDs waveform spreading through air as reference, the reflective single point thickness extraction model can be expressed by Eq.(3):

$$d = \frac{c \cdot \Delta t}{2(n - n_0)} \quad (3)$$

Where  $c$  is the light propagation speed in vacuum,  $n$  is the refractive index of the tested CMC sample,  $n_0$  is the refractive index of the air ( $n_0=1$ ),  $\Delta t$  is the time delay between air and the sample.

Extracting multiple sets of waveforms from the reflection image with no defect, as shown in Fig.7. Taking the reflected beam peak time node as the time delay, THz detection beam peak time node through the air is  $t_{air}=164$  ps, THz detection beam peak time

node through the bottom of sample is  $t_{\text{sample}}=194.1$  ps, so the time delay is  $\Delta t=t_{\text{sample}}-t_{\text{air}}=30.1$  ps. According to the Eq.(3), we can calculate the refractive index of the sample<sup>[10]</sup>,  $n=1.15$ .

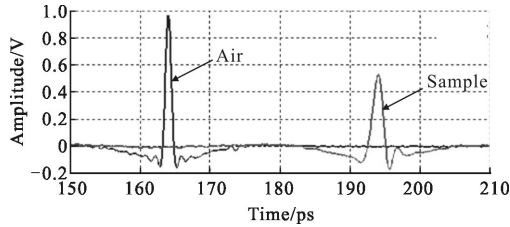


Fig.7 THz-TDs waveforms of the sample with no defect

Once the refractive index of the sample is obtained, the thickness of the defect can be calculated by the reflective single point thickness extraction model. Firstly, extracting the time domain waveforms from the first group defects, as shown in Fig.8,  $t_{\text{defect1}}=192.6$  ps,  $t_{\text{defect2}}=192.1$  ps,  $t_{\text{defect3}}=187.0$  ps. Then we can calculate the depth of the defects:

$$\text{depth}_n=d-d_n \quad (4)$$

Where  $\text{depth}_n$  is the depth of the defects,  $d$  is the thickness of sample,  $d_n$  is the thickness of the defects.

We can obtain the depth of the defects:  $\text{depth}_1=1.4$  mm,  $\text{depth}_2=1.8$  mm,  $\text{depth}_3=7.0$  mm. The results are in accordance with the actual size of the defects.

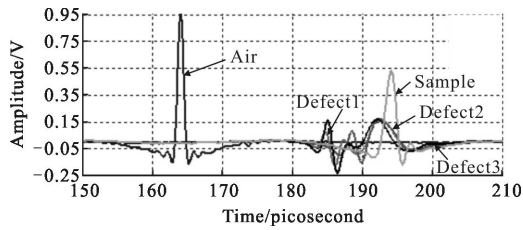


Fig.8 THz-TDs waveforms of the first group

Calculating the first group lateral hole-type defects diameter based on B-Scan diagram, as shown in Fig.9, whose horizontal axis represents the pixels, and longitudinal axis represents the flight time. Similarly, we can obtain THz-TDs waveforms of the second group, as shown in Fig.10, and calculate the theoretical size of defects  $\phi_4=6.4$  mm,  $\text{depth}_4=7.2$  mm;  $\phi_5=5.8$  mm,  $\text{depth}_5=5.0$  mm;  $\phi_6=3.6$  mm,  $\text{depth}_6=4.2$  mm. In this experiment, we set the scanning step at 0.2 mm.

In Fig.11, the number of pixels of the first group defects are  $N_1=27$ ,  $N_2=25$ ,  $N_3=20$ . For Eq.(5):

$$\phi=0.2*N \quad (5)$$

So the cylindrical hole-type defects diameter in the first group respectively are:  $\phi_1=5.4$  mm,  $\phi_2=5.0$  mm,  $\phi_3=4.0$  mm.

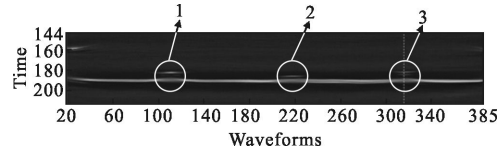


Fig.9 B-SCAN diagram of the first group

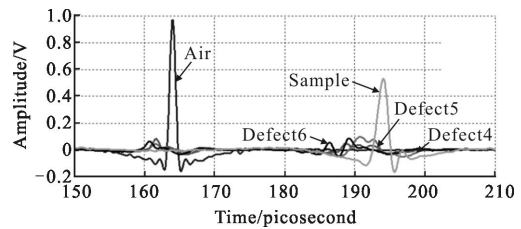


Fig.10 THz-TDs waveforms of the second group

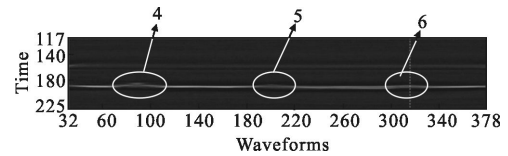


Fig.11 B-SCAN diagram of the second group

It can be seen that: (1) We can calculate the depth information (in testing direction) accurately with the single point detection model; (2) The B-SCAN diagram can show the depth information of the two group of prefabricated defects clearly, and estimate the position information and dimension information, however, there are errors compared with the actual size of the two group defects, so the B-SCAN diagram can't calculate the size of the defects accurately because of the marginal effect.

It is worth noting that the amplitude loss is very serious at the test of defect. This is because that the 3D morphology of the defect could be equivalent to a cylindrical lens which would change the path of the detecting pulse. In this case, very little part of the amplitude would be received which would make the amplitude loss meaningless for this part of experiment. Actually, defects are usually in irregular shapes.

Mostly, the influence of defects in irregular shapes to Terahertz pulse is similar to the influence of lens to light beam. On the one side, the irregular surface would reflect the detect pulse to directions which is beyond the detection range; on the other side, the defect itself would cause interference by changing the path and the shape of the Terahertz wave which is similar to the Gaussian beam.

Nevertheless, no matter how the amplitude loses<sup>[11]</sup>, as long as the Terahertz wave is not completely interdicted which means that the detector is still able to distinguish the Terahertz pulse from the noise, the time delay is with the ability of carrying the size information of the defect as shown in B-SCAN diagram.

The size of the defect in Z-direction (the testing direction) is still able to be calculated according to the time delay. Also the location, shape and size of the defect in X-Y plane is able to be obtained by imaging.

Furthermore, the sample was subjected to stress of some extent due to the production progress of defects, so a crack might be formed within the material, which would be found in the scanning images of the defects materials. Thus the time-domain and frequency-domain waveform of the suspected crack are analyzed, the result of which reveals massive detected amplitude loss from which we can determine that the crack defect do exists. This shows the brittle ceramic matrix composites is vulnerable to external forces, it also reflects the excellent detecting ability of the terahertz time-domain spectroscopy detection.

In addition, uneven distributions of time delay and amplitude loss are noticed during the experiments. Therefore, further experiments are carried on based on the time-delay-related detecting model (ignoring the error brought by scattering and uneven reflection) to evaluate the homogeneity of the sample.

### 2.3 Porosity distribution analysis

3 pieces of ordinary sample with different density

which are 30 mm in thickness are placed under the best detection range (waist of the Gaussian beam) to process the transmission experiment. The obvious absorption ranges of CMC sample in frequency (0.2–1.7 THz) is selected as the interest region to calculate in detecting.

Density distribution analysis of the samples are done according to the extracted optical parameters<sup>[12]</sup> and the time delay. Shown in Fig.12, the 3D image is generated to describe the non-uniformity distribution status of a part of the sample (about 40 mm×24 mm). The result of which demonstrates that the uneven density distribution in CMC is ubiquitous. Variance curves are applied to describe the discreteness of the density distribution, shown in Fig.13.

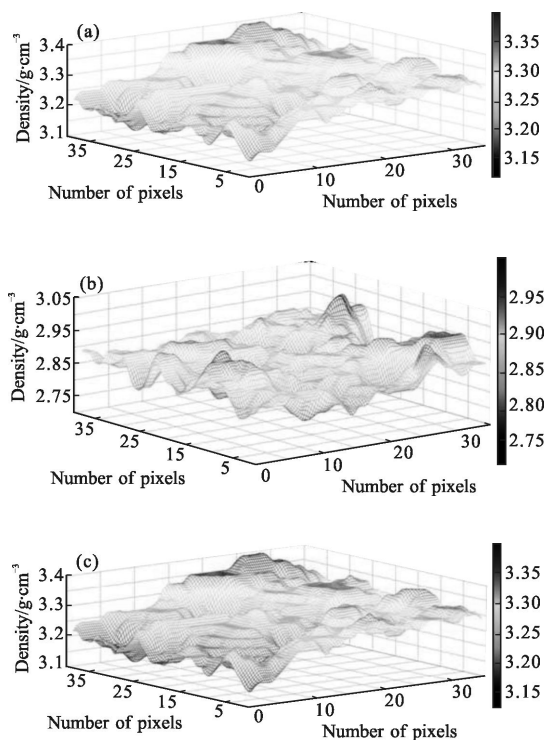
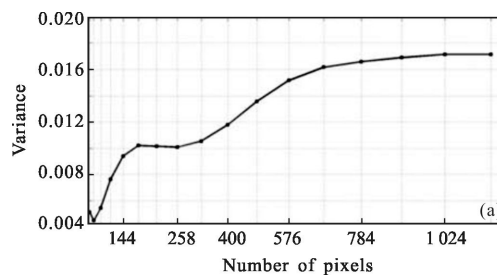


Fig.12 3-D density distribution of 3 samples with different densities



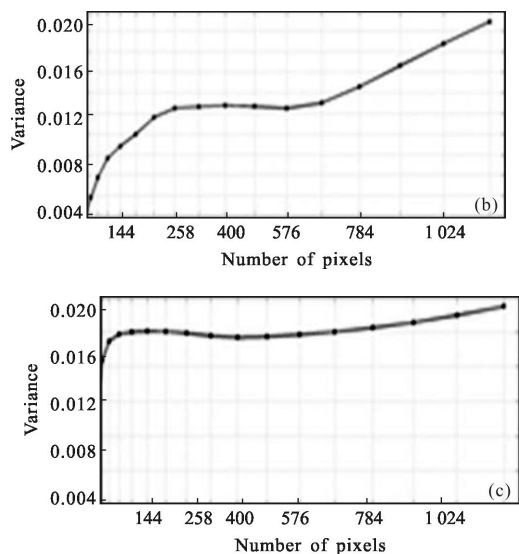


Fig.13 Variance curves for density distribution of the 3 samples

The variance curves are drawn by selecting square areas of increasing sizes. Each pixel is a 0.5 mm×0.5 mm square. Seen from the Fig.13, inhomogeneous density distribution could be found in ordinary materials of different density. This ubiquitous feature would absolutely affect the performance of the material or even cause accidents. This phenomenon can be termed as the uneven porosity distribution because of the osteoporosis internal structure of CMC. The test results, to a certain extent, improve the material quality evaluation index which has guiding significance for exploring material characteristics.

It should be noticed that uneven reflection and scattering effect caused by the surface roughness of the material conditions have impact on the carrying capacity of Terahertz wave. Therefore, imaging result, time delay and amplitude variations should be comprehensively taken into account as evaluation criteria in spectral analysis, making the result of quantitative detection more accurate.

### 2.4 Limitations

The experiments still exposes certain limitations: Position of irregular defects in Z direction (perpendicular to the scanning plane) is still an open question due to lacking of reference. This is because the rough surface of the defects could not supply the

detector an echo which is obvious enough to be identified from the noise. This problem is believed to be solved by the development of Terahertz pulse coding technology and signal processing technology. Besides, the samples selected in our experiments are cubes in regular shape which is short of universality in engineering. The detection of special-shaped samples depends on the combining of precision topography measurement and detecting in normal direction by the employment of robot arms.

It is worth mentioning that excellent achievements has been made in single kind of material with Terahertz Continuous Wave (CW) imaging. But there are always different kinds of assembled materials need to be tested which is quite common in modern industry manufacturing. So the time domain spectroscopy with wider bandwidth is more suitable for materials with different spectral characteristics rather than CW.

### 3 Conclusion

In this paper, CMC is taken as the sample. Based on electromagnetic wave transmission theory, detection model of thickness at single point and extraction model of optical parameters like refractive index or absorption coefficient are established. A quantitative detection method is proposed according to the differences of the flight time and amplitude loss between terahertz spread through the sample and air layer of the same geometrical thickness. Validating experiments have been designed and performed, in which the testing and evaluation of the sample are studied from the angel of porosity (or density) distributions and holes.

The experiment result indicates that terahertz wave has a good carrying capacity of information. The defects would be distinguished and analyzed according to the time-frequency analysis of detection signal and reference signal. Convincing validation is completed that CMC has an uneven distribution of porosity. Quantitative testing results of detection could

be given for the hole-type defects. Confirmatory experiment also reflects the brittleness of the material, which demonstrates the feasibility of the application of time-domain Terahertz spectroscopy in quantitative detection on both theory and engineering projects.

**References:**

- [1] Winfree W P, Anastasir F, Seebo J P. Crack detection in sprayed on foam insulation with pulsed terahertz frequency electromagnetic waves [J]. *Review of Progress in Quantitative NDE*, 2006, 92(3): 148–189.
- [2] Wang Tiejun, Yuan Shuai, Chen Yanping, et al. Intense broadband THz generation from femtosecond laser filamentation [J]. *Chinese Optics Letters*, 2013, 1130705530 (1): 11401–350.
- [3] Murrill S R, Jacobs E L, Moyer S K, et al. Terahertz imaging system performance model for concealed-weapon identification [J]. *Applied Optics*, 2008, 47(9): 1286–1297.
- [4] Wilmink G J, Grundt J E. Current state of research on biological effects of terahertz radiation [J]. *Journal of Infrared, Millimeter, and Terahertz Waves*, 2011, 32 (10): 1074–1122.
- [5] Tan Zhiyong, Gu Li, Xu Tianhong, et al. Real-time reflection imaging with terahertz camera and quantum-cascade laser [J]. *Chinese Optics Letters*, 2014, 12 (7): 070401–070403.
- [6] Cai He, Guo Xuejiao, He Ting, et al. Terahertz wave and its new applications[J]. *Chinese Journal of Optics and Applied Optics*, 2010, 15(3): 209–222. (in Chinese)
- [7] Ye Quanyi, Yang Chun. Recent progress in THz sources based on photonics methods[J]. *Chinese Optics*, 2012, 5(1): 1–11. (in Chinese)
- [8] Li Hongguang, Yang Hongru, Xue Zhanli, et al. Terahertz radiation detection of low temperature blackbody based on narrowband spectral filter method [J]. *Optics and Precision Engineering*, 2013, 21(6): 1410–1416. (in Chinese)
- [9] Deng Hu, Shan Liping, Zhang Zelin. Transmission characteristics of water vapor based on different transmission distance [J]. *Infrared and Laser Engineering*, 2015, 44 (3): 979–984. (in Chinese)
- [10] Luo Zhiwei, Gu Xinan, Zhu Weichen, et al. Optical properties of GaSe: S crystals in terahertz frequency range [J]. *Optics and Precision Engineering*, 2011, 19 (2): 354–359. (in Chinese)
- [11] Yang Jing, Zhao Jiayu, Guo Lanjun. Study of terahertz radiation from filamentation induced by ultrafast laser pulses [J]. *Infrared and Laser Engineering*, 2015, 44(3): 996–1007. (in Chinese)
- [12] Li Zongyang, Tan Lan, Yuan Yuan. Theoretical research on amplification characteristic of terahertz wave parametric oscillation [J]. *Infrared and Laser Engineering*, 2014,43(8): 2650–2655. (in Chinese)